Wireless Power Transmission using Finite Difference Time-Domain Analysis

[1]Prof.B.Somashekar, [2]Dr.Ganapathy D Moger, [3] Dr.N.Lakshmipathy, [4]Dr.Joshi Manohar V, [5] Dr.Yogesh G S
[1]Research Scholar, East Point College of Engineering & Technology, Bangalore
& Associate Professor, Dr.T.Thimmaiah Institute of Technology, KGF
[2]Associate Professor, Dept. of EEE, RRIT, Bangalore
[3] Professor & HOD, Dept of EEE Dr.T.Thimmaiah Institute of Technology, KGF
[4]Professor & HOD, Dept. of EEE, Presidency University, Bangalore
[5]Professor & HOD, Dept. of ECE, East Point College of Engineering & Technology, Bangalore

Abstract:

We present a way to simulate a wireless power transfer (WPT) device of the electromagnetic induction kind. The time-domain finite-difference approach served as the foundation for this simulator. The simulation and experimental findings agreed well enough to cut down on computing time. With this simulation, it is anticipated that a transient response study of WPT devices will be available in the future. In order to conduct the electromagnetic (EM) analysis required to ascertain the proper transmitter geometry and electrical field and magnetic field distribution for wireless power transmission, this paper describes the creation of a numerical simulation approach. Limited-Difference Complex electromagnetic issues can be solved with a strong computational approach called Time-Domain (FDTD) analysis. This study implements FDTD analysis using MATLAB programming to assess wireless power transmission (WPT) systems.

Finite-Difference Time-Domain (FDTD) analysis is a powerful computer tool for solving complicated electromagnetic issues. This study leverages MATLAB programming to perform FDTD analysis on wireless power transmission (WPT) systems running at utility frequency (50Hz). The major focus is on the propagation properties of electromagnetic fields within several core materials—ferrite and silicon—and how they affect power transfer efficiency. The MATLAB-based FDTD study shows considerable changes in electromagnetic field distribution and intensity between ferrite and silicon cores. Ferrite cores outperform silicon cores in terms of power losses and transfer efficiency, because to their higher magnetic permeability and lower conductivity. Although silicon cores have larger losses, they give useful insights into material behavior under utility frequency operations.

Key Words:

FDTD analysis, MATLAB programming, wireless power transmission, 50Hz utility frequency, ferrite core, silicon core, electromagnetic field, power transfer efficiency, electromagnetic simulation, computational electromagnetic.

Introduction:

In a few years, wireless power transmission (WPT) for EV charging is anticipated to be available for widespread usage. The majority of EV producers will use an electromagnetic Using an 85 kHz high-frequency power source, the induction type WPT enables coil shrinkage. On the other hand, power losses in high-frequency converters and inverters often rise with frequency. In order to handle high frequency losses, considerable research has concentrated on inverter design and control strategies [1-4]. As an easy way to lower power losses in these power semiconductor devices, we have suggested a super-low-frequency WPT system [5, 6]. In many situations, the inverter is not required, such as when using 60 Hz as the standard utility frequency. In addition, for vessels and airplanes, a 400-Hz power

Direct usage of the power supply frequency is an option. The fact that very low frequency does not heat metallic items is another benefit of using it. Get into the area of transmission. Electricity may therefore be transmitted through a reinforced concrete wall using a super-low-frequency WPT [5].For electromagnetic field modeling, the finite-element method (FEM) for frequency-domain analysis and the finite-difference time-domain (FDTD) approach are frequently employed [7–10]. Using weighted residuals, the FEM is an indirect approach for solving Maxwell's equations. The FDTD technique, on the other hand, converts Maxwell's equations into finite-difference equations and offers a straightforward solution. A high spatial resolution computer simulation is required to precisely portray the form of the magnetic core in the construction of a WPT device. FEM may be used for WPT research [11–13], but we also want to replicate electromagnetic fields that are transitory, as those that occur when a metallic item enters the transmission area. Even so, the The FDTD approach may be used to lower frequencies; however, it is mostly employed for high-frequency electromagnetic waves. However, the Courant–Friedrichs–Lewy (CFL) condition causes the time step to shorten when the wavelength is considerably bigger than the analysis region, or when the frequency is low [14]. As a result, there are more processing iterations, which lengthens calculation times. This is the reason why an electromagnetic induction-type WPT device has never been simulated using the FDTD approaches. The technique known as wireless power transfer, or WPT, has

shown promise in a number of fields, including consumer electronics, electric cars, and medical implants. The fundamental idea behind WPT is the use of electromagnetic fields to transport electrical energy without the need for physical connections. It is crucial for these systems to provide effective power transmission, which is determined by a number of variables such as operating frequency, transmitter and receiver coil design, and core component material composition. There are particular potential and constraints for WPT systems operating at the 50Hz utility frequency. In order to examine the performance of WPT systems running at this frequency, this work focuses on applying the Finite-Difference Time-Domain (FDTD) approach, a potent computational methodology for solving Maxwell's equations. In particular, the study looks at how silicon and ferrite, two distinct core materials, affect power transmission efficiency.

Understanding how electromagnetic fields travel through various materials in detail is necessary for effective wireless power transmission at 50Hz. Ferrite cores are frequently utilized in WPT systems because of their low electrical conductivity and high magnetic permeability. Nonetheless, silicon cores have the potential to be more cost- and availability-effective due to their reduced magnetic permeability. Through the use of FDTD analysis in MATLAB, this study seeks to compare the performance of these two materials. This study's main goal is to model and simulate the electromagnetic behavior of WPT systems with silicon and ferrite cores using MATLAB-based FDTD analysis, then assess the systems' effectiveness and performance at 50Hz. The goal of the study is to determine which core material is most suited for improving WPT systems at utility frequency. The study entails simulating the distribution of electromagnetic fields and the process of power transfer by creating intricate 3D models of the WPT system's component parts and applying the FDTD method in MATLAB. In order to investigate their influence on field propagation and power transfer efficiency, the simulation incorporates the material characteristics of silicon and ferrite. The performance of the two core materials is compared through analysis of the simulation data.

FDTD Analysis

A numerical analysis method called the Finite-Difference Time-Domain (FDTD) method is used to model computational electrodynamics. To solve Maxwell's equations, which describe the behavior of electromagnetic fields, the approach discreteness both space and time. This section describes the FDTD method's theoretical underpinnings, MATLAB implementation, and application to the analysis of wireless power transmission networks.

By utilizing finite differences to approximate the derivatives, the FDTD approach solves Maxwell's curl equations. Maxwell's time-dependent equations are especially well suited for FDTD because they enable the direct computation of field values at later time steps based on earlier values. In order to ensure that the fields evolve appropriately in accordance with Maxwell's equations, the main concept is to build a grid in both space and time where the electric and magnetic field components are computed alternately.

A grid of cells having spatial steps Δx, Δy, Δz, and a temporal step Δt makes up the computational domain. To guarantee precise and stable simulations, the value of Δt must meet the Courant stability criterion. Accurate FDTD simulations require appropriate boundary conditions. In order to reduce reflections from the edges of the computational domain and absorb outgoing waves, perfectly matched layers, or PMLs, are frequently utilized. The simulation receives inputs related to the permittivity, permeability, and conductivity of the core materials. The way that electromagnetic fields interact with materials is determined by these qualities. Using finite difference approximations, the FDTD method updates the electric and magnetic field components at each grid point as it moves through time steps. Iteratively solving Maxwell's curl equations in discrete form is the procedure.

Wireless Power Transfer Circuit

Transmission power and efficiency in magnetic resonance type WPTs, as WiTricity devices, have been predicted using the coupled-mode theory [15, 16]. Regarding the On the other hand, similar circuit analysis has often been utilized for WPTs of the electromagnetic induction type [17, 18]. Because similar circuit analysis simply necessitates the exchange of the quality factor (Q) and coupling coefficient (k) across processors, we determined that it satisfied our processing speed targets [19]. Fig. 1 depicts the analogous circuit for the induction WPT system. The principal C_1 and secondary C_2 capacitors, which serve as leakage inductance compensators, were linked in series, or series-series (SS) mode, with their corresponding coils. The WPT framework within the Immittance conversion features are present in SS mode [20]. Consequently, the WPT system in SS mode functions as a constant current supply if a power supply source operates as a constant voltage supply. The load resistance under minimal copper loss circumstances (R_{Lmax}), transmission power under RLmax (Pout), and transmission efficiency under minimum copper loss conditions (η_{max}) may all be all be stated, as indicated in Table 2, using k and Q. (All parameters, with the exception of $\omega 0$, the power supply's angular frequency, are described in the caption for Fig. (1) The main and secondary coil turn ratios are assumed to be 1:1 in these formulae. Since the technique of deriving the equations is comparable, it is not explained here. To the parallel-parallel mode procedure, which is covered in the paper [6]. The R_{Lmax} value cannot be determined in the absence of knowledge of the k and Q variables. The resonant state's capacitors are subject to the same rules. The magnetic coupling coefficient, or k, in this case is the leakage inductance that the capacitors are compensating for, and it cannot be determined from the electromagnetic field in the resonant state. In the resonant state, Q and self-inductance (L) cannot be determined from the electromagnetic field. The main and secondary coil turn ratios are assumed to be 1:1 in these formulae. Since the technique of deriving the equations is comparable, it is not explained here.

To the parallel-parallel mode procedure, which is covered in the paper [6].

As a result, k and Q (or L) values must be obtained beforehand by simulating the non resonance condition in an electromagnetic field. These parameters, however, do not remain constants under temporary circumstances, as variations in the separation between two coils.

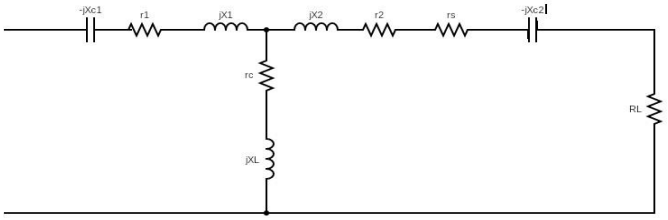

Fig 1 Schematic of the WPT equivalent circuit in SS mode.

Figure 1 shows the schematic of the SS mode WPT equivalent circuit. Primary winding resistance (r_1), secondary leakage inductance (jx_1), primary capacitance ($-jx_{C1}$), secondary winding resistance (r_2), stray load loss resistance (r_s), secondary leakage inductance (jx_2), secondary capacitance ($-jx_{C2}$), core loss resistance (r_c), mutual inductance (jx_L), and load resistance (R_L) are all represented.

Expressions derived from the equivalent circuit Analysis

Primary Capacitor $C_1 = \frac{1}{x_{L1}\ \omega_0}$, $x_{L1} = x_L + x_1$

Secondary capacitor $C_2 = \frac{1}{x_{L2}\ \omega_0}$, $x_{L2} = x_L + x_2$

Q of primary coil $Q_1 = \frac{\omega_0 L_1}{r_1}$

Q of secondary coil $Q_2 = \frac{\omega_0 L_2}{r_2}$

Optimum load resistance $R_{Lmax} = kr_2\sqrt{Q_1 Q_2}$

Maximum efficiency η max = $\frac{1}{1+\left(\sqrt{Q_1 Q_2}\frac{2}{k}\right)} + \frac{2r_{c(k+k-1)}}{Q_2 r_2} + \frac{r_{s(2k+k-1)}}{Q_2 r_2}$

Output current $I_L = jI_{IN}$

Output voltage $V_L = jV_{IN}\eta_{max}$

Input impedance $Z = \frac{x_L^2}{R_{Lmax}}$

Input power $P_{in} = I_{IN}^2 Z$

Output power $P_{inout} = I_L^2 R_{Lmax}$

The equations show that knowing the k and Q values is necessary in order to specify the R_{Lmax} value. For the resonant state, the same holds true for capacitors. Here, the magnetic coupling is denoted by k coefficient, or the leakage inductance compensated by the capacitors, which cannot be determined from the electromagnetic field in the resonant condition. In the resonant state, Q and self-inductance (L) cannot be determined from the electromagnetic field. As a result, k and Q (or L) values must be obtained beforehand by simulating the non resonance condition in an electromagnetic field. Under temporary circumstances, as when the separation between two coils varies, these characteristics are not constants.

Calculation Method

The mimicked WPT device consisted of a silicon-steel magnetic core and enamel-covered copper wire. The simulated magnetic core was a directed silicon-steel plate with 3.5% silicon, the same material utilized in the actual device. We used the manufacturer's μ-H curve to calculate the magnetic permeability (μ) of this steel plate in relation to the magnetic field (H). We overlooked hysteresis in steel plates. The core loss resistance (r_c) was measured for a closed-loop inductor core built of the same material. Difference equations were utilized to calculate the electromagnetic field. To arrange the vectors for electric and magnetic fields around arbitrary two-dimensional coordinates (i, j), assume the electric field and current source (J_e) exist in the z direction and the magnetic field and current source (J_ϕ) exist in the x and y directions, respectively.

The electric field in the z direction (E_z) at any time ($t = n\Delta t$) and position ($i\Delta x$, $j\Delta y$) is expressed as follows: $E_Z(t = n\Delta t, x = i\Delta x, y = j\Delta y) \equiv E_z^n(i, j)$

The electric field equation was derived by centering Maxwell's equations with regard to space and time.

$$E_z^n(i,j) = \alpha E_z^{n-1}(i,j) + \frac{\beta}{\Delta x}\left(H_y^{n-\frac{1}{2}}\left(i+\frac{1}{2},j\right) - H_y^{n-\frac{1}{2}}\left(i-\frac{1}{2},j\right)\right) - \frac{\beta}{\Delta y}\left(H_y^{n-\frac{1}{2}}\left(i,\frac{1}{2}+j\right) - H_x^{n-\frac{1}{2}}\left(i,\frac{1}{2}-j\right)\right) - \beta j_{e,z}^{n-\frac{1}{2}}(i,j) \quad (1)$$

Where,

$$\alpha = \frac{1-\left((\sigma(i,j)\Delta t)/\left(2\varepsilon(i,j)\right)\right)}{1+\left((\sigma(i,j)\Delta t)/\left(2\varepsilon(i,j)\right)\right)} \quad (2)$$

$$\beta = \frac{\left((\Delta t)/\epsilon(i,j)\right)}{1+\left((\sigma(i,j)\Delta t)/2\varepsilon(i,j)\right)} \quad (3)$$

The dielectric constant is denoted by ε, while magnetic conductivity is represented by σ.

J_e represents the current that flows through the primary coil.

The amplitude of a sinusoidal current $I0$ flowing in the z direction at random coordinates can be represented as $J_{e,z}^{n-\left(\frac{1}{2}\right)}$

$$J_{e,z}^{n-\left(\frac{1}{2}\right)}(i,j) = \frac{1}{\Delta x \Delta y} I_0 sin\left(\omega_0\left(n-\frac{1}{2}\right)\Delta t\right) \quad (4)$$

The difference equations for magnetic fields H_x and H_y were determined by differentiating Maxwell's equations, where μ represents permeability. Magnetic cores are typically magnetized by an external magnetic field, while magnetic poles generate magnetic charges. The presence of these charges suppresses the magnetic field in the core, resulting in a self-demagnetization effect. This phenomenon is crucial for electromagnetic induction type WPT. The self-demagnetization effect can be represented as J_ϕ, which corresponds to J_m, as the

magnetic charge density (σ_ϕ) at a magnetic pole is equal to the magnetization. J_m can be determined using the core's magnetic susceptibility and the magnetic field applied to it.

$$H_x^{n+\frac{1}{2}}\left(i,j+\frac{1}{2}\right)=\left(H_x^{n-\frac{1}{2}}\left(i,\frac{1}{2}+j\right)-\frac{\Delta t}{\mu(i,j)\Delta y}\right)X\left(E_z^n\left(i,1+j\right)-E_z^n\left(\frac{\Delta t}{\mu(i,j)}\right)J_{\phi,x}^n(i,j)\right) \quad (5)$$

$$H_y^{n+\frac{1}{2}}\left(j,i+\frac{1}{2}\right)=\left(H_y^{n-\frac{1}{2}}\left(i+\frac{1}{2},j\right)+\frac{\Delta t}{\mu(i,j)\Delta x}\right)X\left(E_z^n\left(i+1,j\right)-E_z^n(i,j)\right)-\left(\frac{\Delta t}{\mu(i,j)}\right)J_{\phi,y}^n(i,j) \quad (6)$$

To improve simulation accuracy, the capacitors and loads connected to the coils are modeled as lumped elements. The FDTD approach allows for the introduction of lumped elements.

The electric field equation. We added the following equation to E_z to link a capacitor C along the z direction at any x-y coordinates.

$$E_z^n(i,j)=E_z^{n-1}(i,j)+\frac{\gamma}{\Delta x}\left(H_y^{n-\frac{1}{2}}\left(i+\frac{1}{2},j\right)-H_y^{n-\frac{1}{2}}\left(i-\frac{1}{2},j\right)\right)-\frac{\gamma}{\Delta y}\left(H_y^{n-\frac{1}{2}}\left(i,\frac{1}{2}+j\right)-H_x^{n-\frac{1}{2}}\left(i,-\frac{1}{2}+j\right)\right) \quad (7)$$

Where

$$\gamma=\frac{\frac{\Delta t}{\epsilon(i,j)}}{1+\left((c(i,j)\Delta z)/\epsilon(i,j)\Delta x\Delta y\right)} \quad (8)$$

The equation below links the resistance R in the z direction at arbitrary x-y coordinates.

$$E_z^n(i,j)=\delta E_z^{n-1}(i,j)+\frac{\xi}{\Delta x}\left(H_y^{n-\frac{1}{2}}\left(i+\frac{1}{2},j\right)-H_y^{n-\frac{1}{2}}\left(i-\frac{1}{2},j\right)\right)-\frac{\xi}{\Delta y}\left(H_x^{n-\frac{1}{2}}\left(i,\frac{1}{2}+j\right)-H_x^{n-\frac{1}{2}}\left(i,-\frac{1}{2}+j\right)\right) \quad (9)$$

Where

$$\delta=\frac{1-\left((\Delta t\Delta z)/2R(i,j)\right)\epsilon(i,j)\Delta x\Delta y}{1+\left((\Delta t\Delta z)/2R(i,j)\right)\epsilon(i,j)\Delta x\Delta y} \quad (10)$$

$$\xi=\frac{1-\left((\Delta t)\right)\epsilon(i,j)}{1+\left((\Delta t\Delta z)/2R(i,j)\right)\epsilon(i,j)\Delta x\Delta y} \quad (11)$$

The wave's propagation towards the PML divides Ez, Hx, and Hy into two components, as shown below.

$$E_z=E_{zx}+E_{zy}$$
$$H_z=H_{xy}+H_{xz}$$
$$H_{zy}=H_{yz}+H_{yx}$$

In the case of a transverse magnetic wave, H_{xz} and H_{yz} are null, as wave propagation in the z direction is not considered. The PML defines both anisotropic conductivity (σ) and anisotropic magnetic conductivity (σ ∗).

$$\frac{\sigma_x}{\epsilon}=\frac{\sigma_x^*}{\mu},\frac{\sigma_y}{\epsilon}=\frac{\sigma_y^*}{\mu} \quad (12)$$

$$E_z^{n+1}(i,j)=\frac{1}{\left(1+\left(\sigma_{x(i)}/\epsilon(i,j)\right)\Delta t\right)}X\left(E_{zx}^n(i,j)+\frac{c\Delta t}{\epsilon_r\Delta x}\left(\zeta H_y^{n+\frac{1}{2}}\right)\left(i+\frac{1}{2},j\right)\right)-\left(\left(\zeta H_y^{n+\frac{1}{2}}\right)\left(i-\frac{1}{2},j\right)\right) \quad (13)$$

$$E_{zy}^{n+1}(i,j)=\frac{1}{\left(1+\left(\sigma_{y(j)}/\epsilon(i,j)\right)\Delta t\right)}X\left(E_{zy}^n(i,j)-\frac{c\Delta t}{\epsilon_r\Delta y}\left(\zeta H_x^{n+\frac{1}{2}}\right)\left(i,\frac{1}{2}+j\right)\right)-\left(\left(\zeta H_x^{n+\frac{1}{2}}\right)\left(i,-\frac{1}{2}+j\right)\right) \quad (14)$$

The equations below represent the difference equations for each component in Equation that meet criteria. The equation includes the speed of light (c), wave impedance (ς), relative boundary permittivity (ε_r), and relative boundary permeability (μ_r).

$$\zeta H_{xy}^{n+\frac{1}{2}}\left(i,j+\frac{1}{2}\right)=\frac{1}{\left(1+\left(\sigma_y\left(j+\frac{1}{2}\right)/\mu(i,j)\right)\Delta t\right)}X\left(\zeta H_{xy}^{n-\frac{1}{2}}\left(i,j+\frac{1}{2}\right)-\frac{c\Delta t}{\mu_r\Delta y}(E_z^n)(i,1+j)\right)-\left(E_z^n(i,j)\right) \quad (15)$$

$$\zeta H_{yx}^{n+\frac{1}{2}}\left(i+\frac{1}{2},j\right)=\frac{1}{\left(1+\left(\sigma_x\left(i+\frac{1}{2}\right)/\mu(i,j)\right)\Delta t\right)}X\left(\zeta H_{yx}^{n-\frac{1}{2}}\left(i+\frac{1}{2},j\right)-\frac{c\Delta t}{\mu_r\Delta y}(E_z^n)(i+1.j)\right)-\left(E_z^n(i,j)\right) \quad (16)$$

Simulation and Experimental Results

Finite-Difference Time-Domain (FDTD) analysis can also be used in Wireless Power Transfer (WPT) systems that use silicon steel components.

FDTD study of a WPT system with silicon steel components entails modeling the geometry, adding material properties, discretizing Maxwell's equations, applying boundary conditions, modeling the electromagnetic source, iterating the solver, and evaluating system performance. This method enables precise simulation and optimization of WPT systems with silicon steel components.

Matlab code is built to analyze the FDTD of electrical and magnetically behavior of wireless power transfer system based on the specifications of the hardware experiment of silicon steel stamping and copper on both sides of the WPT system. The findings of the simulation of FDTD are described below.

Electrical & Magnetic Field Distribution

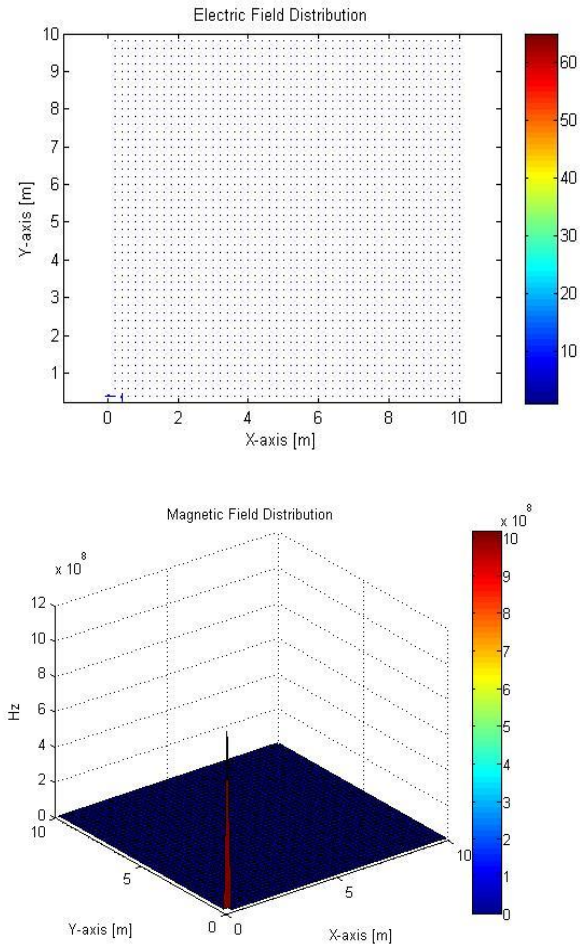

Fig 2: Electrical and Magnetic field distribution

A detailed understanding of the electromagnetic behavior may be obtained by utilizing Finite-Difference Time-Domain (FDTD) data to analyze the electric and magnetic field distributions in a Wireless Power Transfer (WPT) system. This is especially useful when silicon steel components are included. This is how you go about analyzing both fields. We can draw the following conclusions from the electrical field distribution simulation results: the presence of silicon steel components affects the electric field distribution; the electrical field intensity is distributed equally in the given set of boundary conditions in the simulation code; and the electrical field strength is greater near the transmitter and receiver coils. The distribution of the electric field can alter due to the magnetic properties of silicon steel cores and electromagnetic interactions. A number of components, including silicon steel cores, are impacted by the strong magnetic field, which is essential for efficient power transfer. The distribution and concentration of the magnetic field are influenced by silicon steel components. More magnetic flux density and magnetic field steering are possible with silicon steel cores, which improves power transmission efficiency. The way in which magnetic and electric fields are distributed impacts the WPT system's overall efficiency. In order to maximize power transmission efficiency and reduce losses, optimize the design parameters. You may get important insights into the electromagnetic behavior of the WPT system, optimize its design, and verify the accuracy of the simulation by using the FDTD findings to examine the electric and magnetic field distributions.

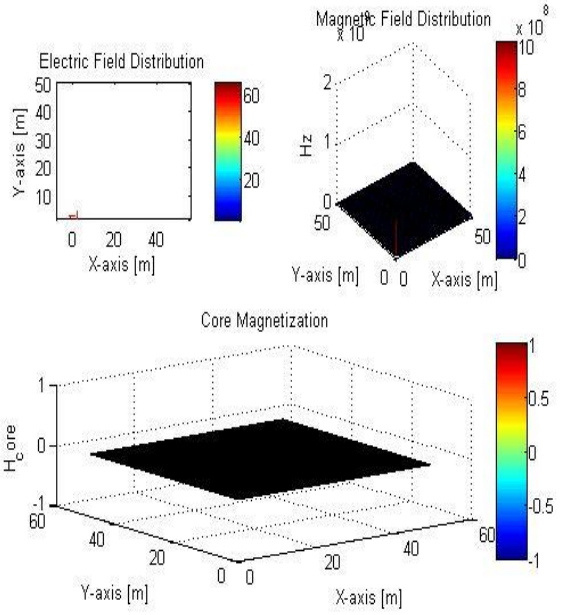

Fig. 3: Core Magnetization

In order to analyze core magnetization in a Wireless Power Transfer (WPT) system using Finite-Difference Time-Domain (FDTD) simulation, one must comprehend how the silicon

steel core material is magnetized by the alternating magnetic field produced by the transmitter coil. The WPT system, comprising the silicon steel core, transmitter coil, and receiver coil, is simulated using FDTD. by defining the simulation domain's shape, material characteristics, and boundary conditions. The simulation takes into account the magnetic properties of the silicon steel core, such as conductivity and permeability (μ). These characteristics affect the core's reaction to the coils' magnetic field. Optimize the WPT system's design parameters to increase efficiency and reduce losses based on the study of core magnetization and losses.

FFT Analysis of Electrical & Magnetic Field Distribution

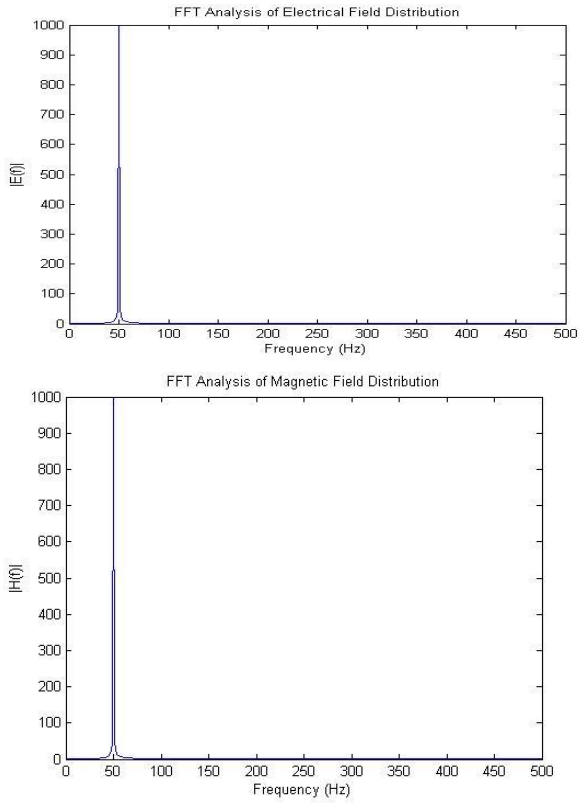

Fig 4: FFT analysis of electrical & Magnetic Field distribution

A better understanding of the electromagnetic behavior of a Wireless Power Transfer (WPT) system with silicon steel and copper wire components operating at 50 Hz and 230V may be gained by doing an FFT analysis of the electrical and magnetic field distributions of the system. To identify the main frequency components, examine the FFT data for the distributions of the magnetic and electrical fields. The fundamental frequency of the input voltage in a WPT system, 50 Hz, is predicted to exhibit significant peaks in both the electrical and magnetic field spectra. The graphs demonstrate how non-linear resonances in the WPT system may be indicated by the presence of harmonics and other frequency components in the spectra. The distribution of the magnetic field is changed by the addition of silicon steel and copper.

Electrical Field Distribution at Transmitter and Receiver side

Electrical field distribution in wireless power transfer (WPT) systems describes the way the electric field is dispersed throughout the transmitter and receiving components. A charged particle feels force per unit charge in an electric field. A computer method for modeling the behavior of electromagnetic fields is called FDTD

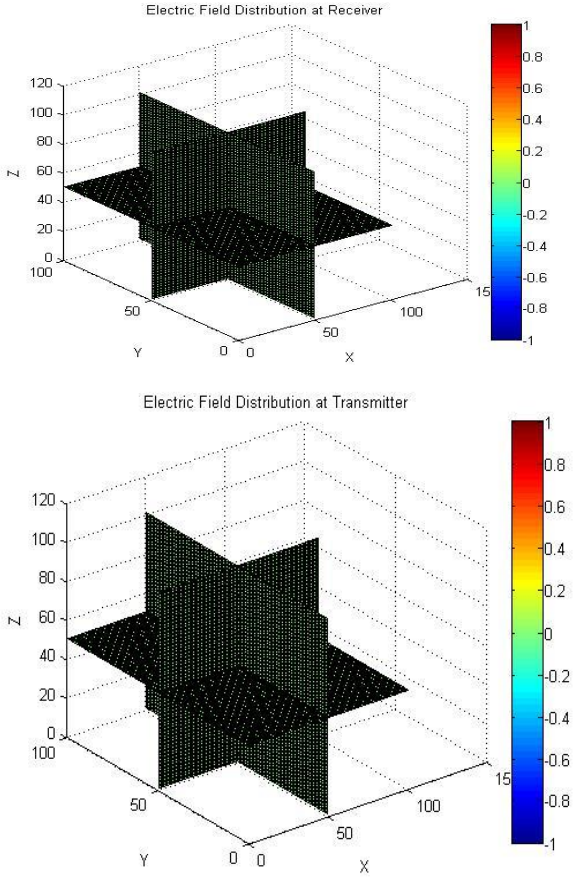

Fig 5: Electrical Field Distribution

In order to model electromagnetic wave propagation, it discretes space and time into a grid and solves Maxwell's equations at each grid point.It is usual for alternating current (AC) power distribution networks to run at a frequency of 50 Hz, which is indicated by wireless power transfer (WPT) at that frequency. An alternating electric field forming around the transmitter coil or antenna would be demonstrated by the

transmitter side FDTD simulation. The alternating current flowing through the transmitter coil produces this electric field. The form of the transmitter coil and the properties of the surrounding materials, such as silicon steel, will dictate the dispersion pattern of the field. The electromagnetic field received from the transmitter would be shown in the FDTD simulation on the receiving end. In the receiver coil, this field produces an alternating voltage. The shape of the receiving coil and the properties of the materials it is surrounded by, such as any silicon steel components, will also affect the distribution of the electric field around it. The copper wire of the receiver coil would effectively transmit the induced voltage to the load, enabling the operation of electronics or battery charging.

Magnetic Field Distribution at Transmitter and Receiver side

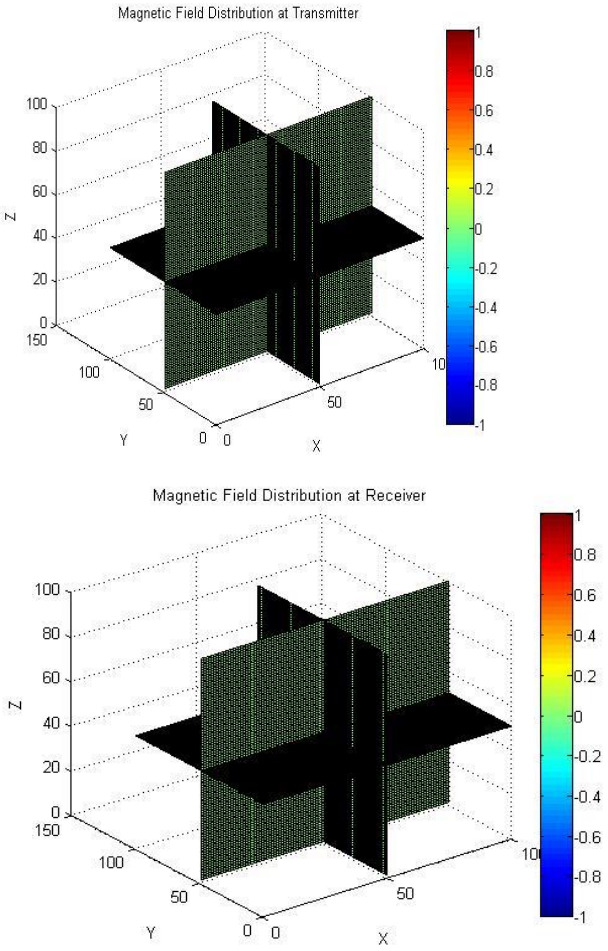

Fig 6: Magnetic Field Distribution

The distribution of magnetic fields in a wireless power transfer (WPT) system, both at the transmitter and receiving ends. A magnetic field is produced by the transmitter's coil or antenna when an alternating current (AC) passes through it. This field stretches out into the surroundings. The distribution of the magnetic field surrounding the transmitter coil may be seen and studied through the use of Finite-Difference Time-Domain (FDTD) simulations. The shape, material properties (silicon steel, for example), and operating frequency (50 Hz) of the coil are all taken into consideration by the simulation. The magnetic field produced by the transmitter on the receiving end creates an alternating voltage in the reception coil. Batteries can be charged or gadgets can be powered by the induced voltage. The distribution of the magnetic field surrounding the receiver coil may be seen using FDTD simulations. The shape of the receiving coil, the material properties (including any silicon steel components), and the distance between the transmitter and receiver are some of the elements that control this distribution. A thorough understanding of the distribution of the magnetic field on the transmitter and receiving sides of a WPT system is provided by FDTD simulations.

The Magnetic and Electric Flux Densities for both Aligned and Misaligned Transmitter and Receiver Coils

To see the magnetic and electric flux densities for aligned and misaligned transmitter and receiver coils, one must comprehend how these densities change with the relative placement of the coils.

The electric flux density is not the underlying problem under normal inductive coupling conditions; rather, it would occur due to any induced currents or voltages. If the coils were part of a capacitive coupling setup, then the electric flux density would be more important, with the lines concentrating in the locations with the largest potential difference or in the gaps between the plates.By comparing the aligned and misaligned setups, it is clear how the alignment affects the flux densities and, consequently, the efficiency of energy transmission between the transmitter and receiving coils.

The input parameters for the three-dimensional (3D) simulation of the distribution of magnetic and electrical fields in both aligned and misaligned systems are listed below. The coil radius is 0.03 cm, the coil thickness is 0.005 cm, the core height is 0.02 cm, the core width is 0.05 cm, and the core length is 0.1 cm. 500 turns of coil; I0 = 1A;

The following figures show the simulation results for the input data that were supplied for the distribution of the magnetic and electrical fields in both scenarios.

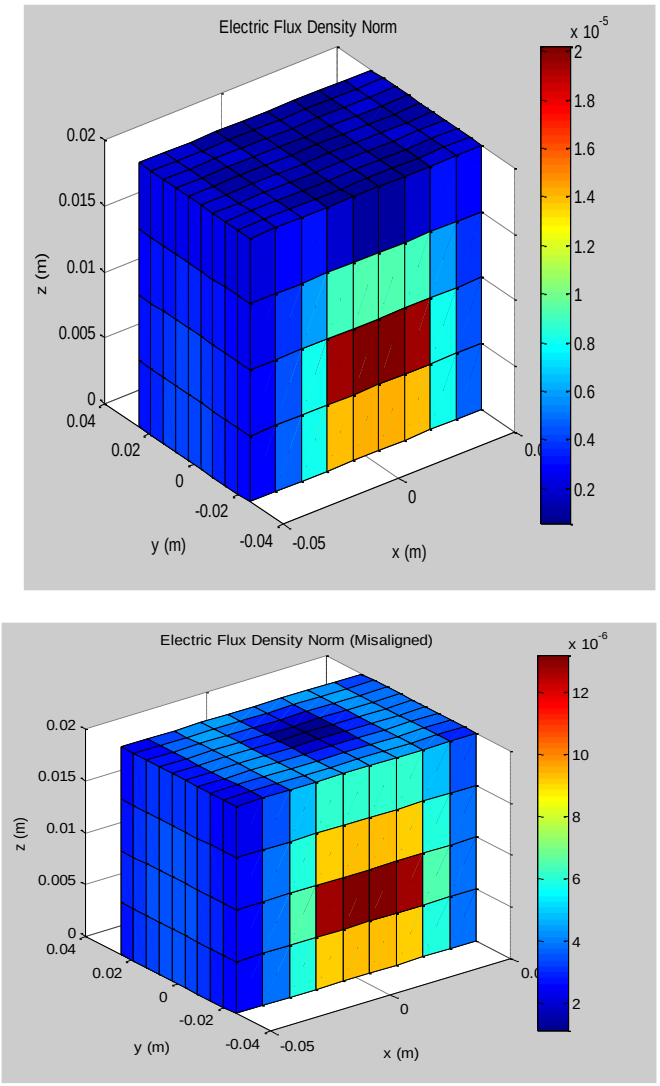

Fig: 7: Electrical Flux Density (Aligned & Misalignment)

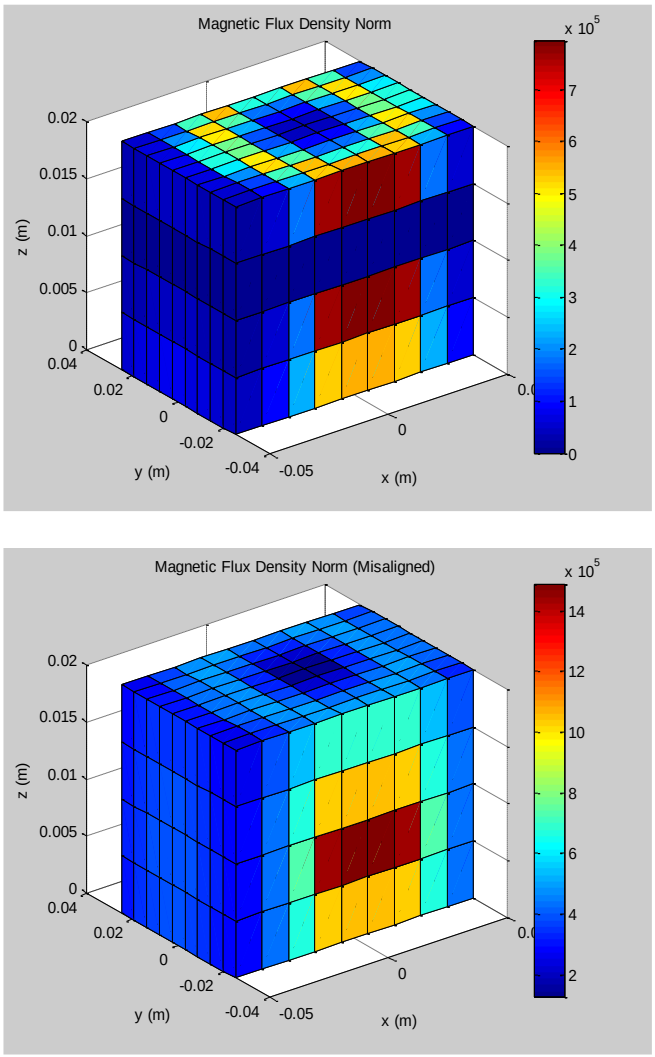

Fig: 8: Magnetic Flux Density (Aligned & Misalignment)

A number of steps are necessary to comprehend and enhance the performance of a wireless power system, one of which is the analysis of synthetic voltage and current signals in the frequency domain using the Fast Fourier Transform (FFT) approach. Wireless power systems, which often use inductive or resonant coupling, can be impacted by noise, harmonics, and other frequency components.Deep insights into a wireless power system's frequency characteristics can be obtained by using FFT analysis to synthetic voltage and current data. Understanding frequency components, harmonics, and noise helps engineers optimize the design, boost efficiency, and ensure dependable operation of wireless power transfer systems.

The input parameter for the FFT, which evaluates fake voltage and current signals in a wireless power system, is as follows: Sample length (samples) Fs = 10,000, sampling frequency (Hz) T = 1/Fs, and sampling period (s) = 1000 Time vector (s) = Fundamental frequency (Hz) * (0:L-1)*T, where f1 = 5. The figure 8 shows the Voltage Spectrum, Current Spectrum, and FFT Analysis Time-Domain Voltage Signal.

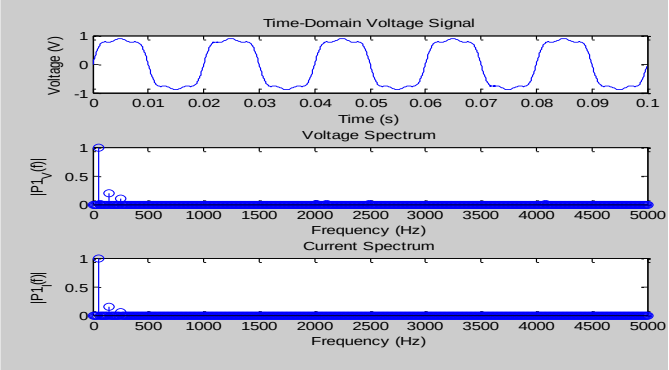

Fig 9: Time-Domain Voltage Signal, Voltage Spectrum & Current Spectrum

FFT Analysis of Electrical & Magnetic Field Distribution

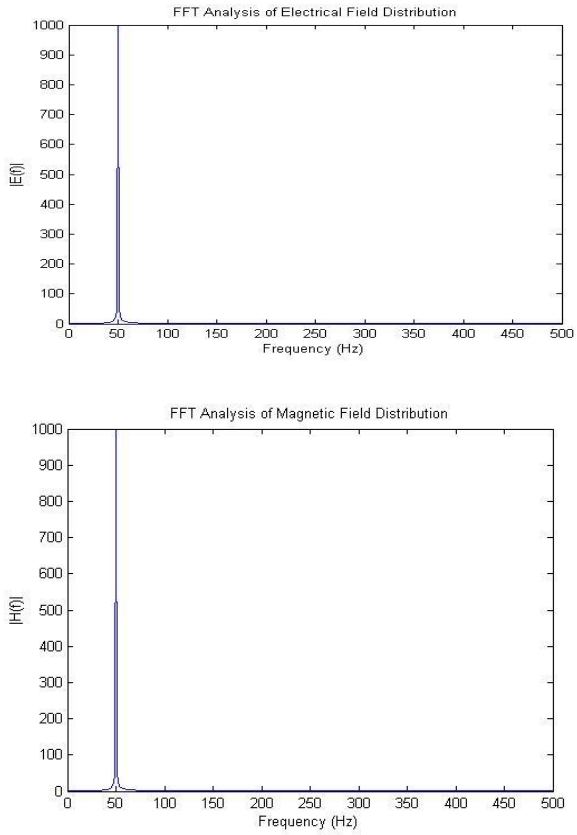

Fig 10: FFT analysis of electrical & Magnetic Field distribution

A better understanding of the electromagnetic behavior of a Wireless Power Transfer (WPT) system with silicon steel and copper wire components operating at 50 Hz and 230V may be gained by doing an FFT analysis of the electrical and magnetic field distributions of the system. To identify the main frequency components, examine the FFT data for the distributions of the magnetic and electrical fields. The fundamental frequency of the input voltage in a WPT system, 50 Hz, is predicted to exhibit significant peaks in both the electrical and magnetic field spectra. The graphs demonstrate how non-linear resonances in the WPT system may be indicated by the presence of harmonics and other frequency components in the spectra. The distribution of the magnetic field is changed when silicon steel and copper are added.

Conclusion:

The performance and efficiency of wireless power transmission (WPT) systems running at a utility frequency of 50 Hz have been greatly improved by the invention of a MATLAB-based simulation of WPT based on the Finite-Difference Time-Domain (FDTD) approach. The objective of this research was to analyze and simulate the electromagnetic behavior of WPT systems by means of a comparison study between silicon and ferrite core materials. The FDTD technique was effectively applied in MATLAB to produce intricate 3D models of the WPT system's constituent parts. The simulations produced a trustworthy depiction of actual conditions by correctly simulating how electromagnetic fields propagate throughout the system.

It was found that the FDTD approach worked well for simulating and evaluating WPT systems. Accurate and stable simulations were made possible by discretizing the computing region and using suitable boundary conditions and material attributes. Field propagation and power transfer over time were seen in a dynamic manner thanks to the iterative time-stepping technique. This study advances the area of wireless power transmission by illuminating how to assess WPT systems at utility frequencies using FDTD analysis. The design and improvement of more effective and affordable WPT systems will be aided by the knowledge obtained from the comparative study of silicon cores. Further study and development in this field can be facilitated by using MATLAB for FDTD simulations, which provides an accessible and adaptable platform.

To build on this work, future investigations might investigate more intricate geometries, investigate different core materials, and incorporate sophisticated boundary conditions to improve the simulation model even further. Confirming the precision and relevance of the results might further benefit from experimental validation of the simulation results. Furthermore, investigating the effects of various system configurations and operating frequencies may offer a deeper comprehension of WPT system behavior. In conclusion, the creation and use of a MATLAB-based FDTD-based simulation for WPT systems has shown to be a useful method for studying and enhancing wireless power transfer. The results highlight the significance of material selection and lay the groundwork for future developments in the area of wireless power transfer.

Reference:

[1] Fu, W., Zhang, B., Qiu, D.: 'Study on frequency tracking wireless power transfer system by resonant coupling'. Proc. IEEE International Power Electronics and Motion Control Conf., 2009, pp. 2658–2663

[2] Kusaka, K., Itoh, J.: 'Reduction of reflected power loss in an AC-DC converter for wireless power transfer systems', *IEEJ J. Ind. Appl.*, 2013, **2**, (4), pp. 195–203

[3] Low, Z. N., Chinga, R., Tseng, R., *et al.*: 'Design and test of a high power high efficiency loosely coupled planar wireless power transfer system', *IEEETrans. Ind. Electron.*, 2009, **56**, (5), pp. 1801–1812

[4] Wang, B., Hu, A. P., Budgett, D.: 'Maintaining middle zero voltage switching operation of parallel–parallel tuned wireless power transfer system under bifurcation', *IET Power Electronics*, 2014, **7**, (1), pp. 78–84

[5] Ishida, H., Furukawa, H.: 'Wireless power transmission through concrete using circuits resonating at utility frequency of 60-Hz', *IEEE Trans. Power Electron.*, 2015, **30**, (3), pp. 1220–1229

[6] Ishida, H., Furukawa, H., Kyoden, T.: 'Development of design methodology for 60 Hz wireless power transmission system', *IEEJ J. Ind. Appl.*, 2016, **5**, (6), pp. 429–438

[7] Goldberg, A. F., Kassakian, J. G., Schlecht, M. F.: 'Finite-element analysis of copper loss in 1-10 MHz transformers', *IEEE Trans. Power Electron.*, 1989, **4**, (2), pp. 157–167

[8] Watson, J. F., Dorrell, D. G.: 'The use of finite element methods to improve techniques for the early detection of faults in 3-phase induction motors', *IEEE Trans. Energy Convers.*, 1999, **14**, (3), pp. 655–660

[9] Sijoy, C., Chaturvedi, S.: 'Calculation of accurate resistance and inductance for complex magnetic coils using the finite-difference time-domain technique for electromagnetics', *IEEE Trans. Plasma Sci.*, 2008, **36**, (1), pp. 70–79

[10] Dalke, R. A., Holloway, C. L., McKenna, P., *et al.*: 'Effects of reinforced concrete structures on RF communications', *IEEE Trans. Electromagn. Compat.*, 2000, **42**, (4), pp. 486–496

[11] Ho, S. L., Wang, J., Fu, W. N., *et al.*: 'A comparative study between novel witricity and traditional inductive magnetic coupling in wireless charging', *IEEE Trans. Magn.*, 2011, **47**, (5), pp. 1522–1525

[12] Duan, C., Jiang, C., Taylor, A., *et al.*: 'Design of a zero-voltage-switching large-air-gap wireless charger with low electric stress for electric vehicles', *IET Power Electron.*, 2013, **6**, (9), pp. 1742–1750

[13] Budhia, M., Covic, G. A., Boys, J. T.: 'Design and optimization of circular magnetic structures for lumped inductive power transfer systems', *IEEE Trans. Power Electron.*, 2011, **26**, (11), pp. 3096–3108

[14] Courant, R., Friedrichs, K., Lewy, H.: 'On the partial difference equations of mathematical physics', *IBM J. Res. Dev.*, 1967, **11**, pp. 215–234

[15] Kurs, A., Karalis, A., Moffatt, R., *et al.*: 'Wireless power transfer via strongly coupled magnetic resonances', *Science*, 2007, **317**, (5834), pp. 83–86

[16] Kurs, A., Moffatt, R., Soljacic, M.: 'Simultaneous mid-range power transfer to multiple devices', *Appl. Phys. Lett.*, 2010, **96**, (044102), pp. 1–3

[17] Imura, T., Hori, Y.: 'Maximizing air gap and efficiency of magnetic resonant coupling for wireless power transfer using equivalent circuit and Neumann formula', *IEEE Trans. Indus. Electron.*, 2011, **58**, (10), pp. 4746–4752

[18] Lee, S. H., Lorenz, R. D.: 'Development and validation of model for 95%- efficiency 220-W wireless power transfer over a 30-cm air gap', *IEEE Trans. Ind. Appl.*, 2011, **47**, (6), pp. 2495–2504

[19] Tohi, T., Kaneko, Y., Abe, S.: 'Maximum efficiency of contactless power transfer systems using k and Q', *IEEJ Trans. Ind. Appl.*, 2012, **132**, (1), pp. 123–124 (in Japanese)

[20] Takanashi, H., Sato, Y., Kaneko, Y., *et al.*: 'A large air gap 3 kW wireless power transfer system for electric vehicles'. Proc. IEEE energy conversion congress and exposition, 2012, pp. 15–20

[21] Berenger, J. P.: 'A perfectly matched layer for the absorption of electromagnetic waves', *J. Comput. Phys.*, 1994, **114**, pp. 185–200

[22] Bi, Z., Wu, K., Wu, C., *et al.*: 'A dispersive boundary condition for microstrip component analysis using the FD-TD method', *IEEE Trans. Microw. Theory. Tech.*, 1992, **40**, (4), pp. 774–777